Original Article
Hepatic fat accumulation and regulation of FAT/CD36: an effect of hepatic irradiation

Gesa Martius[1], Salamah Mohammad Alwahsh[1], Margret Rave-Fränk[2], Clemens Friedrich Hess[2], Hans Christiansen[2*], Giuliano Ramadori[1], Ihtzaz Ahmed Malik[1]

Departments of [1]Gastroenterology and Endocrinology, [2]Radiotherapy and Radiooncology, University Medical Center Goettingen, D-37075 Goettingen, Germany. *Current address: Department of Radiation Oncology, Medizinische Hochschule Hannover, Carl-Neuberg-Straße, 30625 Hannover, Germany.

Abstract: Irradiation is known to induce inflammation and affect fat metabolic pathways. The current study investigates hepatic fat accumulation and fatty acid transportation in a rat model of single dose liver irradiation (25-Gy). Rat livers were selectively irradiated in-vivo (25-Gy), sham-irradiated rats served as controls. Hepatic lipids were studied by colorimetric assays in liver and serum. Intracellular lipids, protein and mRNA were studied by Nile red staining, immunohistology, Western Blot analysis and RT-PCR in liver, respectively. Changes in FAT/CD36 expression were studied in-vitro in a human monocyte cell line U937 after irradiation in presence or absence of infliximab (IFX). Nile Red staining of liver cryosections showed a quick (12-48 h) increase in fat droplets. Accordingly, hepatic triglycerides (TG) and free fatty acids (FFA) were elevated. An early increase (3-6 h) in the serum level of HDL-C, TG and cholesterol was measured after single dose irradiation followed by a decrease thereafter. Furthermore, expression of the fat transporter protein FAT/CD36 was increased, immunohistochemistry revealed basolateral and cytoplasmic expression in hepatocytes. Moreover, apolipoprotein-B100, -C3 and enzymes (acetyl-CoA carboxylase, lipoprotein-lipase, carnitine-palmitoyltransferase, malonyl-CoA-decarboxylase) involved in fat metabolism were induced at 12-24 h. Early activation of the NFkβ pathway (IκBα) by TNF-α was seen, followed by a significant elevation of serum markers for liver damage (AST and GLDH). TNF-α blockage by anti-TNF-α in cell culture (U937) prevented the increase of FAT/CD36 caused by irradiation. Selective liver irradiation is a model for rapid induction of steatosis hepatis and fat accumulation could be triggered by irradiation-induced inflammatory mediators (e.g. TNF-α).

Keywords: Liver, fat accumulation, FAT/CD36, inflammation, cytokines, radiation

Introduction

The liver regulates the metabolism of glucose, proteins and fat. Storage of lipids occurs in hepatocytes as free fatty acids (FFA), triglycerides (TG) and cholesterol, whereby the liver is the main organ which synthesizes TGs and cholesterol [1].

As the liver is the pivotal metabolic organ, hepatic impairment may have serious consequences.

Hepatic steatosis occurs whenever there is an imbalance among the uptake, synthesis, oxidation and secretory pathways of fatty acid metabolism [2]. Sources of fatty acids for hepatic TG synthesis are derived from the plasma non-esterified fatty acids (NEFA) pool and from de novo hepatic lipogenesis (DNL), mainly from glucose [1]. Moreover, a fat-enriched diet also contributes to elevate liver TG and fatty acids.

Fat homeostasis is controlled by a number of factors including different enzymes, transcription factors, membrane and/or intracellular proteins involved in transport, synthesis and degradation of fat [3].

Free fatty acids are taken up by hepatocytes via transport proteins like the transporter fatty acid translocase (FAT/CD36), fatty acid transport protein-1 (FATP-1) and liver fatty acid binding protein (L-FABP) [4].

FAT/CD36 is a membrane bound glycoprotein present on platelets, mononuclear phagocytes,

Table 1. Sequence of the primers used for the realtime PCR

Name	Forward primer	Reverse primer
Acetyl-CoA Carboxylase (ACC-2)	5´-ATGGTCATGCGTTACGGCA-3´	5´-CGGACTCGTTGGTGATGAAGA-3´
Apolipoprotein B100 (ApoB100)	5´-CATGTGTCTGAAGCCATCTG-3´	5´-ACTTGGTTGATACCTCCTCTG-3´
Apolipoprotein C3 (ApoC3)	5´-ACAATCGCTTCAAATCCCTG-3´	5´-ACGGCTCAAGAGTTGGTGTT-3´
β-Actin	5´-GAAATCGTGCGTGACATTAAAGAG-3´	5´-GCGGCAGTGGCCATCTC-3´
Carnitine Palmitoyltransferase 1α (CPT-1α)	5´-CGGTTCAAGAATGGCATCATC-3´	5´-TCACACCCACCACCACGAT-3´
Fatty Acid Transporter/Cluster of Differentiation 36 (FAT/CD36)	5´-GATGTGGAACCCATAACTGGA-3´	5´-CTTTCTCATCGCCAATGGTC-3´
Fatty Acid Transport Protein-1 (FATP-1)	5´-CGCTTCTCAATGTCAACCTG-3´	5´-AAATAGCCGATCATCCATGC-3´
Liver Fatty Acid Binding Protein (L-FABP)	5´-CTGAGGACCTCATCCAGAA-3´	5´-CACCCTCCATCTTAACCAC-3´
Liver Lipoprotease (LPL)	5´-CCCTACAAAGTATTCCATTACC-3´	5´-CCGTGTAAATCAAGAAGGAG-3´
Malonyl-CoA Decarboxylase (MCOAD)	5´-AAGAGTGCCCTCCGTCTGAAA-3´	5´-GCTTTATGAGGAAGGTGCCGA-3´
Mitofusin-2 (Mtf-2)	5´-AGGAAATTGCTGCCATGAAC-3´	5´-GTCTCTTCTCGGTGCAGGTC-3´
Tumor Necrosis Factor α (TNF-α)	5´-ACAAGGCTGCCCCGACTAT-3´	5´-CTCCTGGTATGAAGTGGCAAATC-3´
Ubiquitin (Ubc)	5´-CACCAAGAAGGTCAAACAGGAA-3´	5´-AAGACACCTCCCCATCAAACC-3´
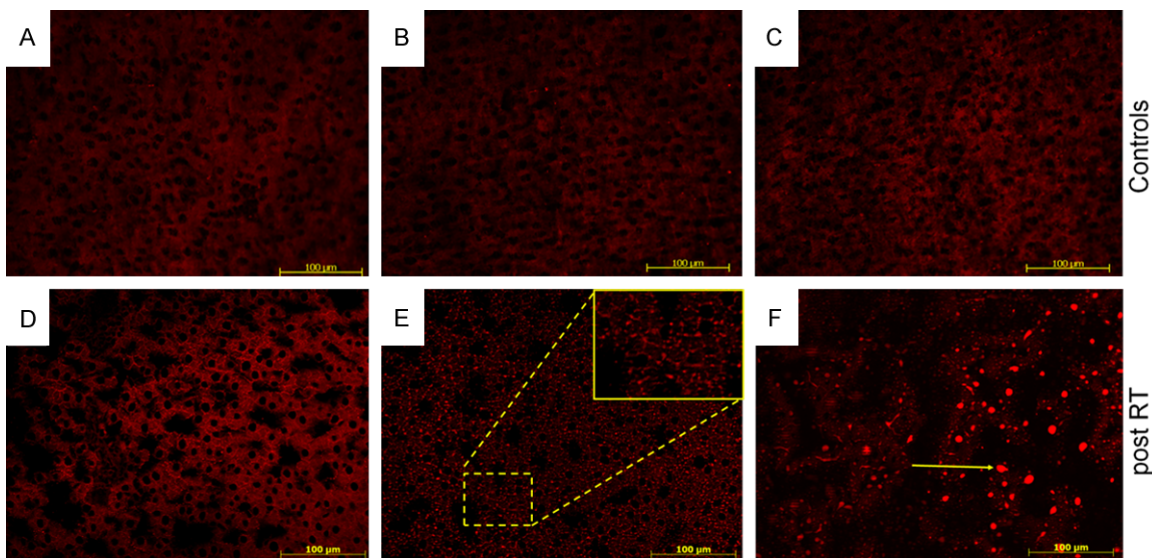
Figure 1. Fluorescent staining of intracellular fat with Nile Red dye in cryosections of livers of 12, 24 and 48 h sham-irradiated controls (A-C) and irradiated rats (D-F). The intracellular accumulation of fat in droplets increased with time. Magnified area is shown in picture E. Arrow in picture F shows lipid droplet. Sections were 5 μm thick. Results show representative picture of three animals and six slides per time point (original magnification, x200).

adipocytes, hepatocytes, and myocytes [3, 5]. A ligand-specific aspect of FAT/CD36 signalling involves its capacity to deliver biologically active lipids to cells. FAT/CD36 is also known to have functions on adipocytes, muscle cells, enterocytes, and hepatocytes as a facilitator of long chain fatty acid transport [6]. There is evidence that fatty acids or oxidized, bind to FAT/CD36, however, the exact mechanism of fatty acid uptake into liver cells remains unclear [7].

In several animal models, ablation of FAT/CD36-mediated lipid uptake into muscle or liver prevented lipotoxicity [8]. In models in which FAT/CD36 was specifically induced in the liver by pharmacologic means or cDNA trans-duction, it may lead to steatosis, which can also contribute to metabolic disorders [7].

In addition, carnitine palmitoyltransferase 1α (CPT1α) is a mitochondrial membrane-localized enzyme that catalyses the key reaction in the metabolism of long chain fatty acyl-CoA by transporting long chain fatty acids from the cytoplasm into mitochondria [9]. Malonyl-CoA decarboxylase (MCOAD) is highly expressed in the liver [9] and also takes part in the degradation of fatty acids.

Radiation therapy involves the use of high-energy rays to treat local or regional malignancies either alone or in combination with modali-
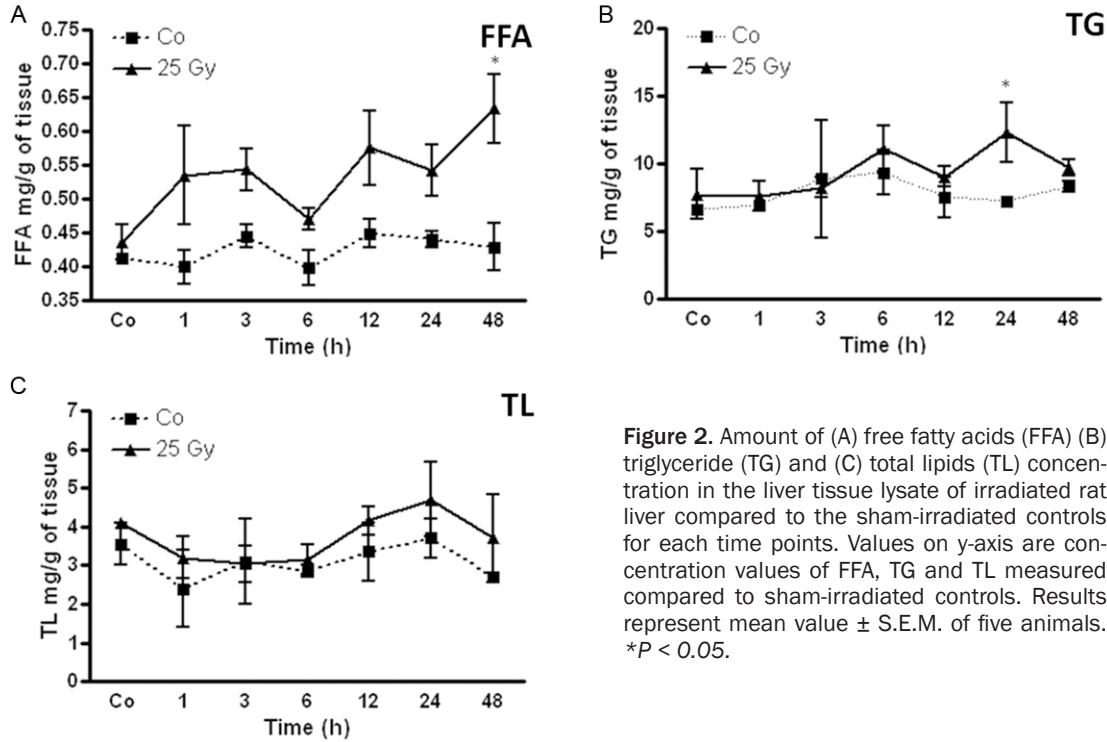
Figure 2. Amount of (A) free fatty acids (FFA) (B) triglyceride (TG) and (C) total lipids (TL) concentration in the liver tissue lysate of irradiated rat liver compared to the sham-irradiated controls for each time points. Values on y-axis are concentration values of FFA, TG and TL measured compared to sham-irradiated controls. Results represent mean value ± S.E.M. of five animals. *$P < 0.05$.

ties such as chemotherapy or surgery. Therapeutic radiation causes both, acute and chronic toxicity in normal tissues [10]. Indeed, radiation-induced liver disease (RILD) is a serious clinical complication [11], mainly due to vessel damage. Radiation-induced inflammation is known to be mediated by cytokines [12]. Furthermore, free radicals such as reactive oxygen species (ROS) are generated after irradiation in irradiated tissue, and cells which are chemically very active are prone to oxidative stress [10]. Moreover, ionizing radiation is recently reported to alter the gene or protein expression of fat metabolism pathway in parallel to accumulation of fat in adipose tissue of rat [13]. However, effect of targeted liver radiation has been not investigated so far.

In our previous work, we have shown that single-dose irradiation of rat liver induces periportal inflammation and changes the gene expression of proteins including those of iron metabolism and inflammatory mediators [14]. As molecular mechanisms underlying inflammatory events during obesity are poorly defined, we extended our previous knowledge and investigated whether single dose liver irradiation could trigger the intracellular fat accumulation in the liver. Additionally, we analysed the changes in gene expression of fat metabolism proteins after irradiation.

Material and methods

Materials

All chemicals used, were of analytical grade and purchased from commercial sources as follows: real-time polymerase chain reaction (PCR) primers, M-MLV reverse transcriptase, reverse transcription buffer, 0.1 M dithiothreitol (DTT), Platinum SYBR green qPCR UDG mix were from Invitrogen (Carlsbad, USA); dNTPs, Protector RNase inhibitor, Klenow enzyme, primer oligo (dT) 15 for complementary DNA (cDNA) synthesis, and Salmon sperm DNA were from Roche (Penzberg, Germany); Hybond N nylon membranes were purchased from Amersham Pharmacia Biotech (Amersham, UK), 4,6-diamidino-2-phenylindole (DAPI) from Southern Biotech (Birmingham, USA). All other reagents and chemicals were from Sigma-Aldrich (St. Louis, USA) or Merck (Darmstadt, Germany).

Animal model

Male Wistar rats of about 200-250 gram body weight were purchased from Harlan-Winkelmann (Brochen, Germany). A rat model for selective liver irradiation was established using CT planned single organ irradiation as described before [15]. Briefly, a planning CT- scan
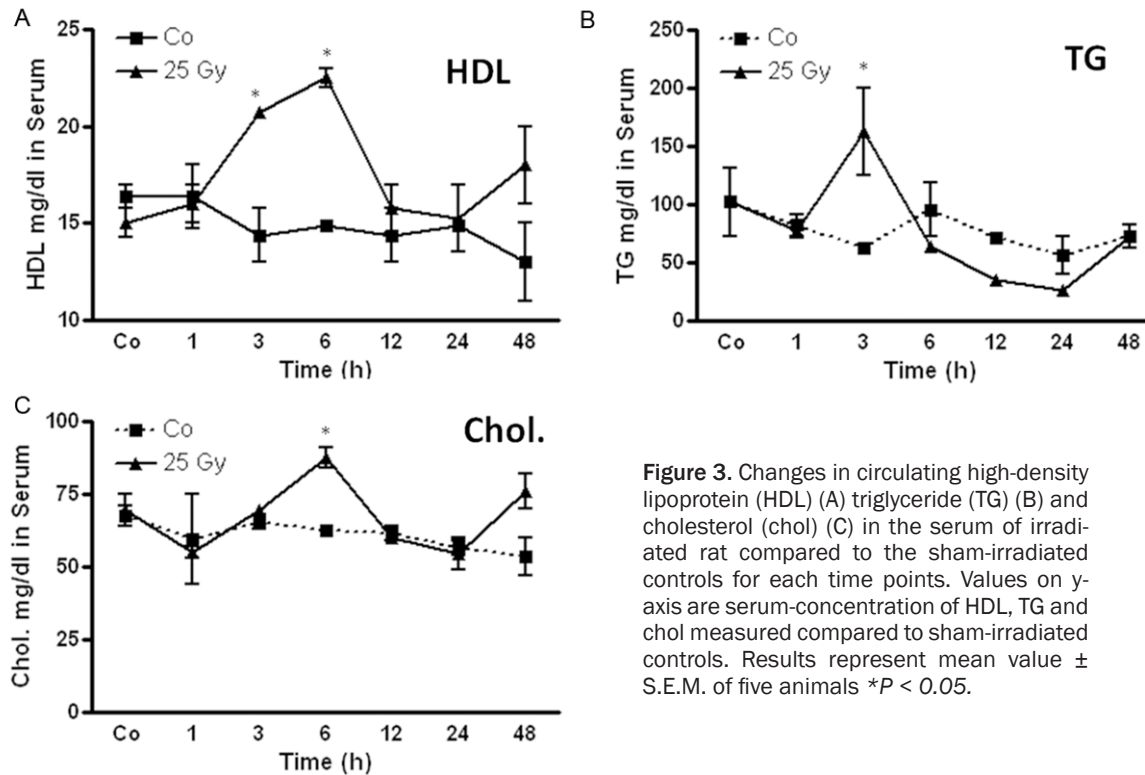
Figure 3. Changes in circulating high-density lipoprotein (HDL) (A) triglyceride (TG) (B) and cholesterol (chol) (C) in the serum of irradiated rat compared to the sham-irradiated controls for each time points. Values on y-axis are serum-concentration of HDL, TG and chol measured compared to sham-irradiated controls. Results represent mean value ± S.E.M. of five animals *P < 0.05.

(Siemens, Erlangen, Germany) was done on each anesthetized rat *i.p.* [90 mg/kg ketamine (Intervet, Unterschleißheim, Germany), 7.5 mg/kg xylazine 2% (Serumwerk Bernburg AG, Bernburg/Saale, Germany)] to delineate the livers of the animals. The margins of the liver were marked on the animal's skin, and a dose distribution was calculated. Livers were irradiated selectively with 6 MV photons (dose rate of 2.4 Gy/min) using a Varian Clinac C accelerator (Varian Medical Systems, Palo Alto, USA). A dose of 25-Gy was delivered using an AP/PA treatment technique. Sham-irradiated control animals were handled similarly but were not irradiated. Treated animals and sham-irradiated controls were killed humanely 1, 3, 6, 12, 24 and 48 h after irradiation. All animals received humane care in accordance to the German Law for the Protection of Animals and the institutional guidelines. The treatment of the rats, and the experiments were approved by the local committee on animal welfare.

Histopathological examination

Unfixed cryostat liver sections (5 μm) from irradiated rats and sham-irradiated controls were stained by Nile Red (Sigma-Aldrich, St. Louis, USA) to study the histology of irradiated-liver tissues compared to sham-irradiated controls.

Nile Red-stained slides were observed by using an Axiovert 200 M epifluorescence microscope (Zeiss, Jena, Germany). Immunofluorescence staining was also performed as described before [14] for FAT/CD36 by using a monoclonal antibody (Abcam, Cambridge, UK) and Alexa Fluor® 555 goat anti-rat rhodamin-coupled was used as secondary antibody (Invitrogen, Carlsbad, USA). Non-immune serum was used as negative control.

Lipid profile and transaminase analysis in serum and liver tissue after irradiation

Blood samples and liver tissues were collected from rats at the studied time points. The plasma levels of TG, total cholesterol, and high-density lipoprotein containing cholesterol (HDL-C) and the activity of liver transaminases aspartate aminotransferase, (AST) and glutamate dehydrogenase (GLDH) were determined by utilizing the automated systems of the central laboratory of the Institute of Clinical Chemistry in University Medical Centre Goettingen. Frozen liver portions (ca. 100 mg) were homogenized in 5% Triton X-100 (Merck, Darmstadt, Germany). TG and FFA concentrations were determined by commercially available kits (BioAssay Systems, Hayward, USA).
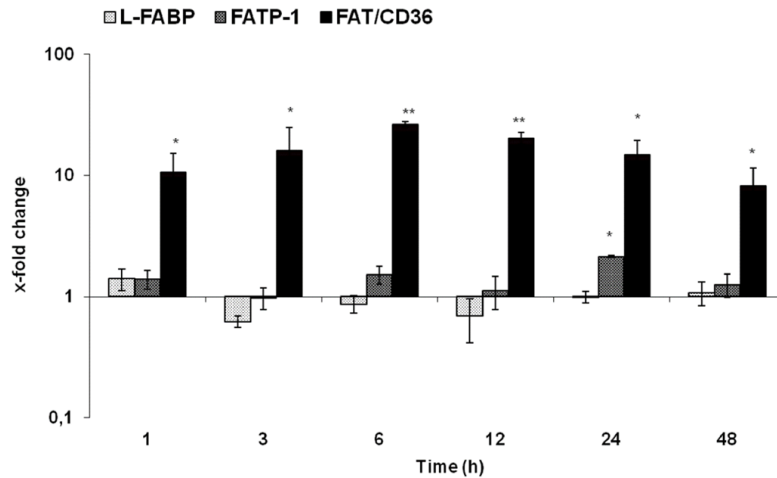
Figure 4. qRT-PCR analysis of total RNA isolated from rat liver after irradiation. Data are shown as fold-changes in mRNA expression of fat transport proteins (L-FABP, FATP-1, and FAT/CD36) at various time-points relative to sham-irradiated controls for each time-point. qRT-PCR was normalized by using two housekeeping genes: β-actin and ubiquitin. Results represent means ± S.E.M. of five experiments; *P < 0.05 n = 5.
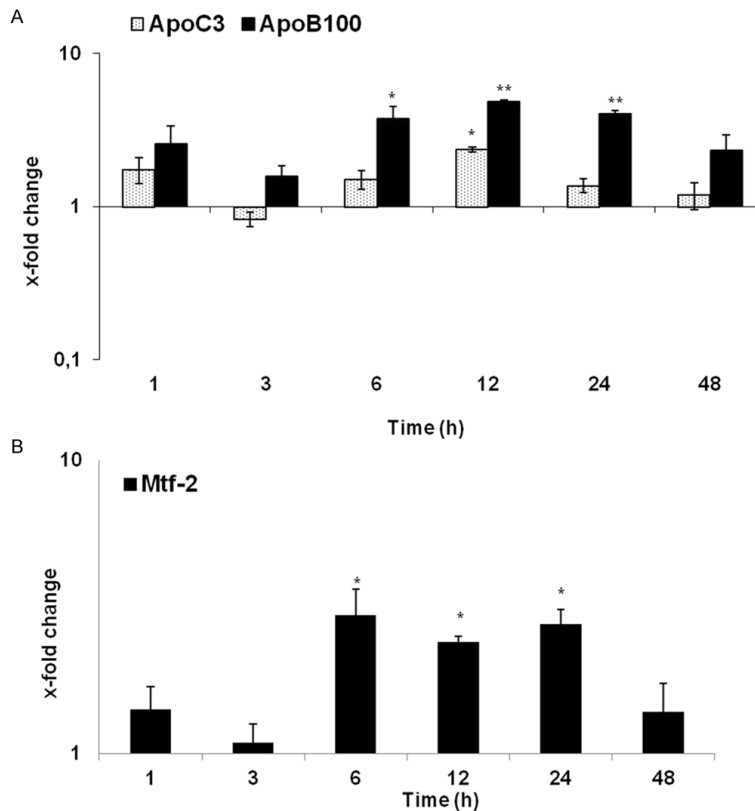
Figure 5. qRT-PCR analysis of total RNA isolated from rat liver after irradiation. Data are shown as fold-changes in mRNA expression of membrane proteins ApoC3, ApoC3 (A) and Mtf-2 (B), that are involved in fatty acid metabolism at various time-points relative to sham-irradiated controls for each time-point. qRT-PCR was normalized by using two housekeeping genes: β-actin and ubiquitin. Results represent means ± S.E.M. of five experiments; *P < 0.05, n = 5.

Lipid quantity was analysed by the Bligh and Dyer method of lipid isolation using chloroform/methanol [16].

RNA isolation and real-time PCR analysis

Total RNA from the livers of irradiated and sham-irradiated rats was isolated after homogenization in guanidine isothiocyanate (Sigma-Aldrich, St. Louis, USA) by the CsCl ultracentrifugation method as described previously [17].

For real-time PCR, reverse transcription of the extracted RNA samples was performed using a Superscript kit from Invitrogen (Carlsbad, USA). Briefly, cDNA was generated by reverse transcription of 1 μg of total RNA using 100 nM of dNTPs, 50 pM of primer oligo dT15, 200 U of moloney murine leukaemia virus reverse transcriptase (M-MLV RT), 16 U of protector RNase inhibitor in RT buffer and 2.5 μl of 0.1 M DTT; real time PCR was performed using an ABI prism 7700 sequence detection system (Applied Biosystems, Darmstadt, Germany) as described elsewhere [14].

β-actin and ubiquitin were used as housekeeping genes. The results were normalized to the housekeeping gene and fold change expression was calculated using threshold cycle (Ct) values. Primer sequences are given in **Table 1**. All primers were synthesized by Invitrogen (Carlsbad, USA).
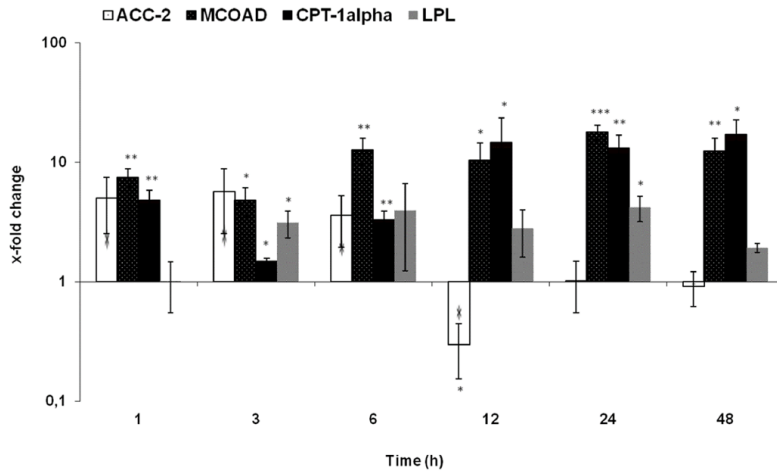
Figure 6. qRT-PCR analysis of total RNA isolated from rat liver after irradiation. Data are shown as fold-changes in mRNA expression of membrane proteins that are involved in fatty acid metabolism. Fold-change expressions of ACC-2, MCOAD, CPT-1α and LPL at various time-points relative to sham-irradiated controls for each time-point. qRT-PCR was normalized by using two housekeeping genes: β-actin and ubiquitin. Results represent means ± S.E.M. of five experiments; *P < 0.05, n = 5.
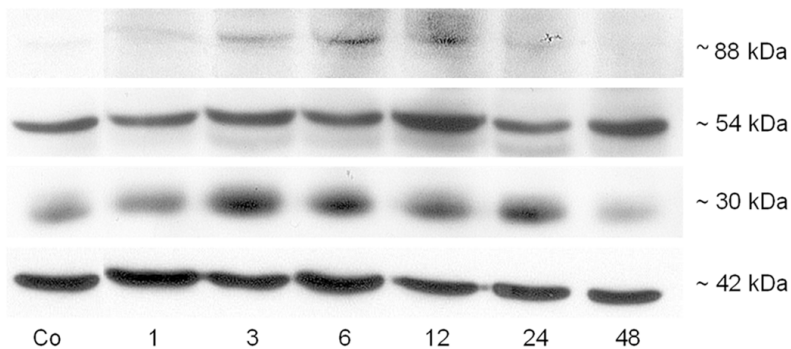
Figure 7. Western blot analysis of total protein from rat liver by using anti-FAT/CD36 after irradiation at different time points. Three bands, ~88 (active isoform), ~54 (inactive isoform) and ~30 kDa (short isoform) were detected after irradiation in rat liver. â-actin (~42 kDa) was used as a loading control. Results are representative of three experiments.

Protein extraction from liver tissue and cells

About 50 mg frozen tissue or cells were homogenized with an Ultra-turrax TP 18/10 (Cole-Parmer, Vernon Hills, USA), three times for 10 s each, in 10 vol 50 mM TRIS-HCl buffer, pH 7.4, containing 150 mM sodium chloride, 1 mM EDTA, 1% Triton X-100, 1 mM phenylmethane sulfonyl-fluoride (PMSF), 1 mM benzamidine, 1 mg/ml leupeptin, 10 mM chymostatin, 1 mg/ml antipain, and 1 mg/ml pepstatin A. The entire procedure was carried out at 4°C. Crude homogenates were passed five times through a 22G needle attached to a syringe and centrifuged for 5 min at 10,000 g, at 4°C. The protein

concentration was determined in supernatants by using the BCA (bicinchoninic acid) protein assay reagent kit (Pierce, Rockford, USA). Aliquots of the homogenates were stored at -20°C until further used for Western blot analysis.

Western blot analysis

Samples of 50 μg proteins were applied per well and subjected to polyacrylamide gel electrophoresis using NuPAGE 4-12% Bis-Tris Gel (Invitrogen, Carlsbad, USA) under reducing conditions as described previously [18]. After electrophoresis, the proteins were transferred to Hybond-ECL (enhanced chemiluminescence) nitrocellulose membranes. Immunodetection was performed according to the ECL Western blotting protocol described before [18]. The antibodies used in this study were, monoclonal anti- FAT/CD36 (Abcam, Cambridge, UK), polyclonal anti-IκBα (Abcam, Cambridge, UK), monoclonal anti-TNF-α (Abcam, Cambridge, UK). β-actin (Sigma-Aldrich, St. Louis, USA) was used for equal loading.

Culture and treatment of promonocytic cell line U-937

U-937 promonocytic cells were seeded at $2x10^5$ cells/ml in RPMI 1640 medium containing 10% (v/v) heat-inactivated fetal calf serum, 2 mM/l L-glutamine, 1 mM/l sodium pyruvate and 1 mM of non-essential amino acids, and cultured at 37°C in an atmosphere of 95% air, 5% CO_2 as described previously [19]. In a second set of experiments, U-937 promonocytic cells were administrated with irradiation (8 Gy) or stimulated with either human TNF-α (10 ng/ml) (Roche, Penzberg, Germany), in the presence of antibody against human TNF-α inflix-
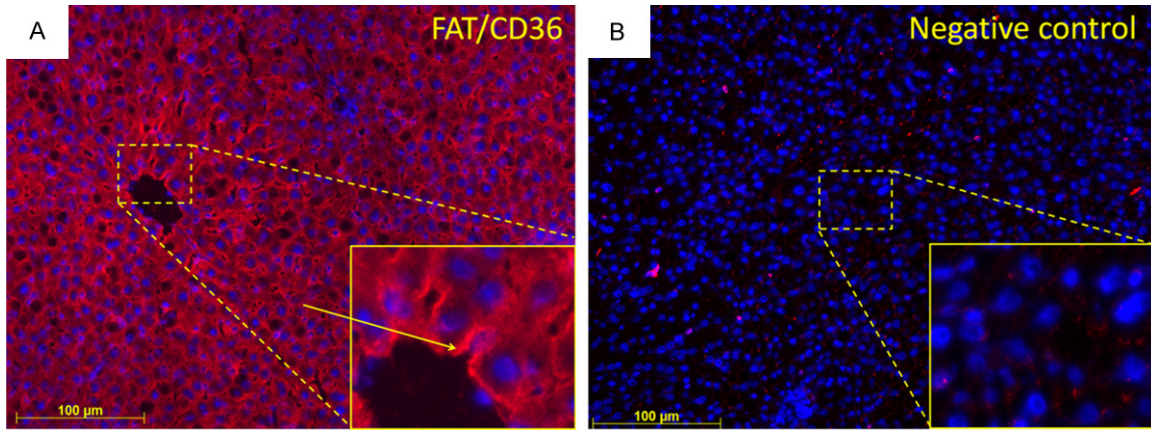
Figure 8. Immunofluorescent staining of liver sections with monoclonal antibody directed against FAT/CD36 followed by fluorescent immunodetection with labeled secondary antibody (red). A. FAT/CD36-positive cells with an arrow which points to basolateral localization, inlet shows higher magnification; B. Negative control, inlet shows higher magnification. Nuclear counterstaining was done with DAPI. Results shows representative picture of three animals (original magnification, x200).

imab (Remicade, 1000 μg/ml) (MSD, Munich, Germany).

Statistical analysis

The data were analysed using Graph pad Prism 4 software (San Diego, USA). All experimental errors are shown as S.E.M. Statistical significance was calculated by student T-test. Significance was accepted at *P < 0.05*.

Results

Accumulation of fat content in rat liver after irradiation

Nile Red staining showed an increase in fat droplets in cryosections of irradiated (**Figure 1D-F**) rat liver after 12, 24 and 48 h. Fat droplets were mainly stained red within hepatocytes and were increasing in size after irradiation in comparison to corresponding sham-irradiated (A-C) control. The maximum fat droplet accumulation was detected at 48 h after irradiation in rat liver (**Figure 1F**).

Change in free fatty acid (FFA), triglyceride (TG) and total lipids (TL) level in rat liver after irradiation

An early (1 h) increase in the FFA level was detected after irradiation compared to sham-irradiated controls in rat liver. The FFA remained above control level throughout the course of the study with a maximum increase at 48 h

(0.63 ± 0.05 mg/g vs. control 0.43 ± 0.035 mg/g).

An elevated pattern for triglycerides (TG) was also observed in rat livers with a peak at 24 h (12.4 ± 2.2 mg/g vs. control 7.3 ± 0.3 mg/g) after irradiation compared to sham-irradiated control rats. However, only minor changes were measured in total lipid content after irradiation (**Figure 2**).

Change in high-density lipoprotein (HDL), triglyceride (TG) and cholesterol (chol) levels in rat serum after irradiation

The HDL level was significantly increased after irradiation compared to sham-irradiated controls (17 ± 0.1 mg/dl) in rat liver. The maximum increase was found at 6 h (22 + 0.5 mg/dl) followed by decrease after 24 h. A similar pattern was also observed for cholesterol with a maximum at 6 h (87.5 ± 3.5 mg/dl vs. control 67 ± 3.5 mg/dl). A significant elevation of TG-serum levels was measured at 3 h (163 ± 37.5 mg/dl vs. control 62.8 ± 4.8 mg/dl) in rat liver after single dose irradiation. The level of TG was reduced after 6 h and remained significantly below control level at 12 h (35 ± 2.3 mg/dl) and 24 h (26 ± 3.5 mg/dl) (**Figure 3**).

Radiation-induced changes of fat metabolism transcripts in liver tissue

Using real-time PCR analysis, mRNA expression from irradiated liver tissue was examined at 1,
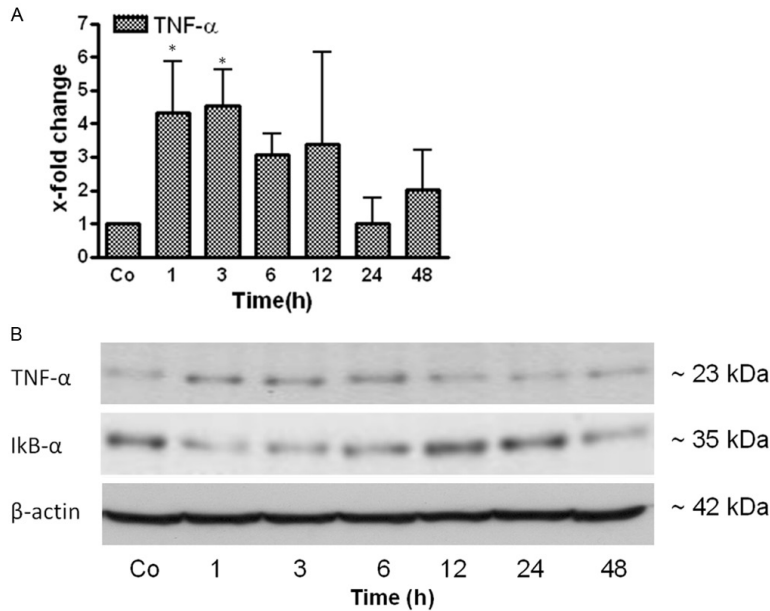
Figure 9. qRT-PCR and Western blot analysis from total RNA and total protein of rat liver after irradiation respectively. A. Fold change in mRNA expression of TNF-α in irradiated rat liver at different time points (1-48 h) related to sham-irradiated controls for each time point. qRT-PCR was normalized by using two housekeeping genes: β-actin and ubiquitin C. Results represent mean value ± S.E.M. of five animals *$p < 0.05$. B. Western blot analysis of protein from rat liver after irradiation by using antibodies specific for TNF-α (upper) and IêBá (middle). β-actin (lower) was used as a loading control. Results are representative of three experiments.

their expression remained above control levels until 48 h. Likewise, ApoC3 gene expression increased early with its peak at 12 h after irradiation. The strongest increase could be seen at 6, 12 and 24 h after treatment (**Figure 5**).

Enzymes: A quick (1 h) and early change in gene expression of ACC2, MCOAD and CPT-alpha was detected after irradiation. The most pronounced increase was detected in gene expression of MCOAD (17.8-fold) at 24 h and CPT-alpha (17-folds) at 48 h and LPL (4.2-fold) at 24 h. The expression of these three genes remained significantly upregulated throughout the course of the study. However, a significant reduction at 12 h was detected in the gene expression of ACC-2 (3.3-fold) (**Figure 6**).

3, 6, 12, 24 and 48 h after irradiation. Gene expression was normalized to corresponding sham-irradiated controls and compared to the expression of ubiquitin.

Fat transport proteins: An early (1 h) significant increase was detected in FAT/CD36 at mRNA level. The most significant upregulation was found at 6 h (26.4 folds) after irradiation. It remained significantly elevated until 48 h after irradiation. The increase of FAT/CD36 was highest after rat liver irradiation among all studied genes. Furthermore, a mild increase in the gene expression of FATP-1 and L-FABP was detected by RT-PCR (**Figure 4**).

Membrane proteins: The examined membrane proteins apolipoprotein C3 (ApoC3), apolipoprotein B100 (ApoB100) and mitofusin-2 (Mtf-2) were up-regulated after irradiation at every measured time point. Gene expression of membrane proteins started to increase early after irradiation. The maximum upregulation was observed for Mtf-2 at 6 h (3-fold) followed by ApoB100 at 12 h (4.8-fold) at transcript level,

Changes in FAT/CD36 protein level in rat liver by western blot analysis

Western blot was performed to analyze the time dependent protein content in irradiated vs. sham irradiated control samples. It is known that FAT/CD36 is built as a non-active form of 54 kDa and is then post-translational glycosylated to its active form of 88 kDa [20]. The antibody detected 3 different antigens which are a 54 kDa, an 88 kDa and a 30 kDa protein. Similar to what was observed at RNA level, using antibody against FAT/CD36 in the irradiated liver tissue, an increased level of FAT/CD36 was detected with a maximum at 12 h for the active and inactive form and a maximum at 3 h for the short isoform. The protein level of all isoforms of FAT/CD36 decreased after 12 h (**Figure 7**).

Localization of FAT/CD36 protein by immuno-fluorescent staining

Immunofluorescent staining of irradiated rat liver section with an antibody against FAT/CD36
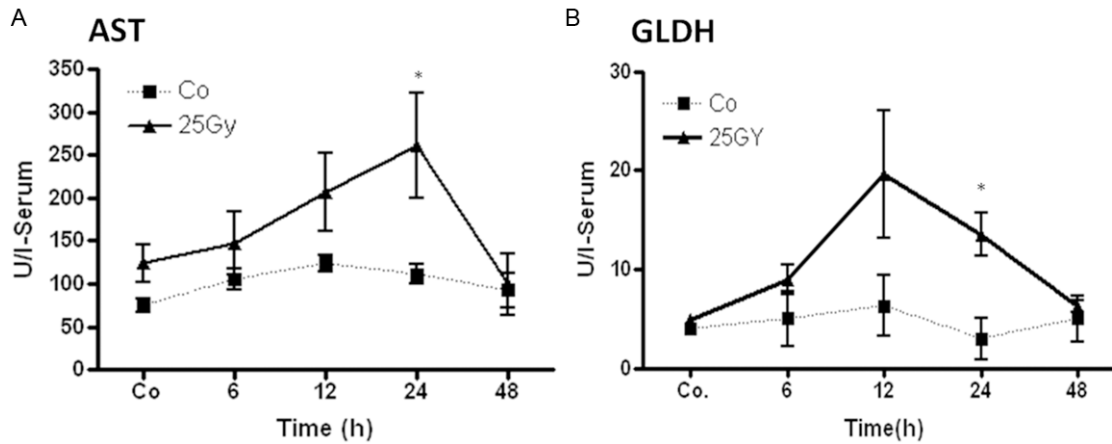
Figure 10. Measurement of aspartate transaminase (AST) and glutamate dehydrogenase (GLDH) concentrations in rat serum after single dose liver irradiation related to sham-irradiated controls for each time point. Results represent means ± S.E.M. of five experiments; *P < 0.05, n = 5.

was performed. A fluorescent signal for FAT/CD36 was found in the basolateral membrane and the cytoplasm of hepatocytes in rat liver (**Figure 8A**). The expression of FAT/CD36 was equally distributed in the liver tissue. The negative controls showed no positive staining of FAT/CD36 (**Figure 8B**).

Real time PCR analysis of TNF-α in irradiated rat liver

The mRNA expression of TNF-α, a major pro-inflammatory cytokine was analyzed in liver tissue at 1, 3, 6, 12, 24 and 48 h after irradiation using real-time PCR analysis. A quick upregulation of TNF-α (4.3-fold) was detected after 1h with a maximum at 3 h. The gene expression of TNF-α then decreased (**Figure 9A**). The results were further confirmed at protein level by Western blot analysis using a specific antibody against membrane-bound TNF-α. The protein level of TNF-α increased at 1-6 h with a decrease thereafter (**Figure 9B**).

Changes in protein expression of IκBα in the rat liver after irradiation

Phosphorylation of the p65 subunit and degradation of IκBα are known to be associated with activation of the NF-κB classical pathway [21]. In order to analyze the activation of the NF-κB pathway, the transcription factor IκBα (subunit of NF-κB) was analyzed at protein level. IκBα protein was decreased at 1 and 3 h. The level of IκBα returned to basal level afterwards in rat liver after irradiation (**Figure 9B**).

Serum level analysis of aspartate transaminase (AST) and glutamate dehydrogenase (GLDH)

The serum level of AST and GLDH both increased between 6 to 12 h with a maximum at 24 h after irradiation compared to sham-irradiated controls. The concentration of both enzymes decreased thereafter (**Figure 10**).

Modulation of FAT/CD36 protein expression in cultured human monocytic cell line U-937

To investigate the role of TNF-α on FAT/CD36 gene regulation, human monocytic cells U-937 were treated with TNF-α and anti-TNF-α (Infliximab, IFX) in the presence or absence of irradiation. After preliminary experiments using different radiation doses (2, 8, 25 Gy) 8 Gy were chosen, as no greater effect was observed by using 25 Gy.

As previously reported [22], only the mature form of FAT/CD36 at > 95 kDa is detectable in unstimulated U937. Similarly, we have detected a ~102 kDa band by using the specific antibody against FAT/CD36. Furthermore, an increase in protein level of FAT/CD36 was revealed in U-937 cells at 8 h to 24 h after TNF-α or irradiation- as compared to the anti-TNF-α (IFX)- and non-treated control cells. In addition, a synergistic effect on FAT/CD36 induction was observed when TNF-α was administered together with irradiation. The up-regulating effect of irradiation was decreased by addition

8Gy	-	+	-	+	-	+
TNF-α	-	-	+	+	-	-
IFX	-	-	-	-	+	+

A

B   CD36

C

D   β-actin
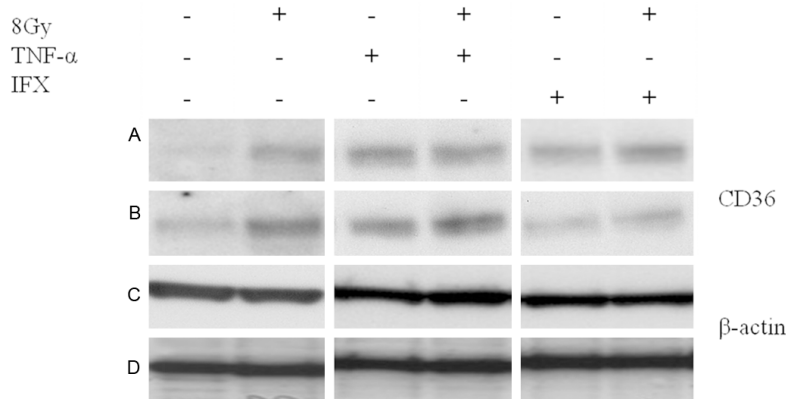
Figure 11. Western blot analysis of total protein isolated from human U-937 cell line by using antibody specific for FAT/CD36 (~102 kDa, active form) after irradiation (8 Gy) and/or tumor necrosis factor-alpha (TNF-α) in the presence/absence of infliximab (IFX) at 8 h (A and C) and 24 h (B and D). â-actin (~42 kDa) was used as a loading control. Results are representative of three experiments.

These results were confirmed at protein level showing an increase in different isoforms of FAT/CD36 after irradiation.

Eventually the accumulation of lipid droplets into the hepatocytes results in hepatic steatosis, [7, 24] which may develop as a consequence of multiple dysfunctions such as alterations in β-oxidation, very low density lipoprotein secretion, and pathways involved in the synthesis of fatty acids [25].

of anti-TNF-α (IFX) to the culture medium (**Figure 11**).

Discussion

Clinical and pathological studies revealed that radiation therapy can produce significant hepatic injury. Radiation-induced liver disease (RILD) has been one of the most important treatment-related complications of hepatic irradiation. The pathomechanisms of radiotherapy-induced hepatic toxicity are not clearly understood [23].

Previously, we showed liver inflammation caused by single-dose-irradiation [14] followed by some fat droplet in the liver by HE-staining method [15]. Therefore, the aim of this project was to ascertain if selective liver irradiation could increase the fat transport into the liver. Furthermore, we studied the changes of genes expression involved in fat transport.

We found an increased fat accumulation by Nile red-staining at 24 and 48 h after liver irradiation. In parallel, TG and FFA levels were also elevated in liver tissue, confirming the accumulation of fat within the cells. An early increase (3-6 h) in serum HDL, TG and cholesterol levels was also found. According to the increased FFA and TG-levels, an increased expression of genes involved in fat metabolism such as ACC-2, LPL, Mtf-2, lipoproteins (ApoB100, ApoC3), and transport proteins (L-FABP, FATP-1, FAT/CD36) was detected at 1-48 h in liver tissue at mRNA level after irradiation. FAT/CD36 showed the highest increase among all studied genes.

The triacylglycerol content of hepatocytes is regulated by the activity of several fat metabolism proteins that facilitate hepatic fatty acid uptake, fatty acid synthesis, and esterification ('input') and hepatic fatty acid oxidation and triacylglycerol export ('output') [26]. ACC-2 regulates the metabolism of fatty acids [27]. An elevated level of ACC-2 in our study indicates *de novo* synthesis of fatty acids and at the same time an increased hydrolysis of fat observed by LPL upregulation which is in accordance to previous studies [28].

On the other hand, in order to transport fatty acids into hepatocytes, several proteins are necessary such as putative fatty acid transporter fatty acid translocase (FAT/CD36), fatty acid transport protein (FATP-1) and liver fatty acid binding protein (L-FABP) which provide the removal of long chain fatty acids from tissues [4, 29-31].

Expression of liver fatty acid binding protein (L-FABP) and transport protein FATP-1 (fatty acid transport protein-1) was least affected by irradiation. These proteins are known to play a role in fatty acid metabolism [32]. However, the role of these proteins in the liver is still not clear. The putative long chain fatty acid transporter FAT/CD36 showed the highest increase in the rat liver after irradiation. Previous studies reported a role of FAT/CD36 in the process of accumulation of triglycerides in the liver which could lead to steatosis [7, 33]. This observation might be most crucial to explain steatosis in our model.

Furthermore, a link between Apo100 and Apoc3 to increased TG has already been documented. These proteins are also known to play a role in fat export [28]. An increased gene expression of these genes could be another reason for steatosis through impaired transport of fatty acids out of liver cells.

Irradiation is known to damage the mitochondrial part of cell [34]. Indeed, disturbance in the hepatic mitochondrial function contributes to hepatic lipid accumulation [35, 36]. Here we observed that the expression of genes involved in mitochondrial biogenesis such as carnitine palmitoyltransferase-1α (CPT-1α) and Mitofusin-2 (Mtf2) was upregulated. CPT-1α is a mitochondrial transmembrane enzyme thought to be rate limiting for long-chain fatty acid entry into the mitochondria for β-oxidation [37-39]. The enzyme malonyl-CoA decarboxylase (MOCAD) is highly expressed in the liver and also takes part in the degradation of fatty acids, it catalyses the decarboxylation of malonyl-CoA to acetyl-CoA [9]. CPT1α and MCOAD are linked by malonyl-CoA; this molecule can inhibit CPT1α and finally the mitochondrial β-oxidation [37].

A highly increased expression of MCOAD and CPT-1α found in the current study points to an altered fatty acid oxidation in the mitochondria due to high amounts of fatty acids within the cells.

Another important aspect of the current and our previous studies was the observation of inflammation with infiltration of neutrophil granulocytes around the portal area [14] and an increase of pro-inflammatory cytokines, mainly TNF-α in serum and liver in the same model [12]. Moreover, the upregulation of TNF-α both at RNA and protein level after irradiation can account for the intense induction of these fat import proteins (e.g. FAT/CD36), indicating a direct effect of the TNF-α, in regulating fat import proteins. In fact, a link between steatosis and inflammation has already been well established [40].

TNF-α is a key player of inflammation and it acts mainly through its transcription factor nuclear transcription factor (NF)-κB which is a pivotal regulator of several genes involved in i.e. inflammation. Phosphorylation of the p65 subunit and the degradation of IκBα are known

to be associated with activation of the NF-κB classical pathway [21, 41]. Induction of TNF-α in parallel to reduction of IκBα level in our study suggests an activation of NF-κB pathway by TNF-α.

To address the question of whether an increase in FAT/CD36 after irradiation induced liver damage could also be due to the direct effect of inflammatory mediators (e.g. TNF-α), a human monocytic cell line U937 (characteristics of macrophages) was therefore cultured and treated with the "major" pro-inflammatory cytokine (TNF-α). Similarly to what is observed in the liver tissue after irradiation, an increase in protein expression of FAT/CD36 was found after TNF-α and/or irradiation administration whereas such an increase was inhibited by the addition of anti-TNF-α into culture medium of U937.

These results are consistent with the view that IFX, by blocking soluble TNF-α, inhibits FAT/CD36 protein level, preventing the increase of FAT/CD36 caused by TNF-α and irradiation in our *in vitro* experiment, a prerequisite for fat transporter into tissue.

The observed effect of anti-TNF-α might contribute to a reduction of inflammatory processes caused by irradiation and/or TNF-α in rat liver, suggesting that a change in gene-expression of FAT/CD36 is also induced by irradiation or/and irradiation induced cytokines.

The unique point of current model is to detect a rapid (within hours) fat accumulation in parallel to liver inflammation after selective single dose liver irradiation, as previously reported fat animal models require long duration (weeks) to establish. Furthermore, these models are also developed by different types of diets such as high-fat or fructose-diet [42-44] which is also difficult to quantify as administrated orally.

Taken together, our current study established a quick hepatic steatosis model by selective rat liver irradiation. Furthermore, transport of fat into the liver could be due to FAT/CD36 which is influenced by cytokines (e.g. TNF-α) produced after irradiation. TNF-α-mediated induction of FAT/CD36 was further confirmed by our *in vitro* experiments. Clinically, regulation of fat metabolism could be an underestimated response in radiotherapy. Further understanding of the fat metabolism before and during radiotherapy

could help to understand hepatic lipid metabolism for the prevention and/or treatment of fat-associated disorders (e.g. Non-alcoholic fatty liver disease). However, prospective studies would need to be performed to correlate fat metabolism dynamics following irradiation to the clinical course of patients developing irradiation-related problems.

Acknowledgements

Disclosure of conflict of interest

None.

Address correspondence to: Dr. Ihtzaz Ahmed Malik, Department of Gastroenterology and Endocrinology, University Medical Center Göttingen, Robert-Koch-Strasse 40, 37075 Göttingen, Germany. Tel: 0049-551-398902; Fax: 0049-551-396921; E-mail: i.malik@med.uni-goettingen.de

References

[1] Donnelly KL, Smith CI, Schwarzenberg SJ, Jessurun J, Boldt MD and Parks EJ. Sources of fatty acids stored in liver and secreted via lipoproteins in patients with nonalcoholic fatty liver disease. J Clin Invest 2005; 115: 1343-1351.

[2] Tilg H and Moschen AR. Evolution of inflammation in nonalcoholic fatty liver disease: the multiple parallel hits hypothesis. Hepatology 2010; 52: 1836-1846.

[3] Silverstein RL and Febbraio M. CD36, a scavenger receptor involved in immunity, metabolism, angiogenesis, and behavior. Sci Signal 2009; 2: re3.

[4] Storch J and Thumser AE. The fatty acid transport function of fatty acid-binding proteins. Biochim Biophys Acta 2000; 1486: 28-44.

[5] Zhang X, Fitzsimmons RL, Cleland LG, Ey PL, Zannettino AC, Farmer EA, Sincock P and Mayrhofer G. CD36/fatty acid translocase in rats: distribution, isolation from hepatocytes, and comparison with the scavenger receptor SR-B1. Lab Invest 2003; 83: 317-332.

[6] Coburn CT, Knapp FF Jr, Febbraio M, Beets AL, Silverstein RL and Abumrad NA. Defective uptake and utilization of long chain fatty acids in muscle and adipose tissues of CD36 knockout mice. J Biol Chem 2000; 275: 32523-32529.

[7] Zhou J, Febbraio M, Wada T, Zhai Y, Kuruba R, He J, Lee JH, Khadem S, Ren S, Li S, Silverstein RL and Xie W. Hepatic fatty acid transporter Cd36 is a common target of LXR, PXR, and PPARgamma in promoting steatosis. Gastroenterology 2008; 134: 556-567.

[8] Yang J, Sambandam N, Han X, Gross RW, Courtois M, Kovacs A, Febbraio M, Finck BN and Kelly DP. CD36 deficiency rescues lipotoxic cardiomyopathy. Circ Res 2007; 100: 1208-1217.

[9] Dyck JR, Berthiaume LG, Thomas PD, Kantor PF, Barr AJ, Barr R, Singh D, Hopkins TA, Voilley N, Prentki M and Lopaschuk GD. Characterization of rat liver malonyl-CoA decarboxylase and the study of its role in regulating fatty acid metabolism. Biochem J 2000; 350: 599-608.

[10] Citrin D, Cotrim AP, Hyodo F, Baum BJ, Krishna MC and Mitchell JB. Radioprotectors and mitigators of radiation-induced normal tissue injury. Oncologist 2010; 15: 360-371.

[11] Shim SJ, Seong J, Lee IJ, Han KH, Chon CY and Ahn SH. Radiation-induced hepatic toxicity after radiotherapy combined with chemotherapy for hepatocellular carcinoma. Hepatol Res 2007; 37: 906-913.

[12] Christiansen H, Sheikh N, Saile B, Reuter F, Rave-Frank M, Hermann RM, Dudas J, Hille A, Hess CF and Ramadori G. X-Irradiation in rat liver: consequent upregulation of hepcidin and downregulation of hemojuvelin and ferroportin-1 gene expression. Radiology 2007; 242: 189-197.

[13] Jo SK, Seol MA, Park HR, Jung U and Roh C. Ionising radiation triggers fat accumulation in white adipose tissue. Int J Radiat Biol 2011; 87: 302-310.

[14] Malik IA, Moriconi F, Sheikh N, Naz N, Khan S, Dudas J, Mansuroglu T, Hess CF, Rave-Frank M, Christiansen H and Ramadori G. Single-dose gamma-irradiation induces up-regulation of chemokine gene expression and recruitment of granulocytes into the portal area but not into other regions of rat hepatic tissue. Am J Pathol 2010; 176: 1801-1815.

[15] Christiansen H, Batusic D, Saile B, Hermann RM, Dudas J, Rave-Frank M, Hess CF, Schmidberger H and Ramadori G. Identification of genes responsive to gamma radiation in rat hepatocytes and rat liver by cDNA array gene expression analysis. Radiat Res 2006; 165: 318-325.

[16] Bligh EG and Dyer WJ. A rapid method of total lipid extraction and purification. Can J Biochem Physiol 1959; 37: 911-917.

[17] Naz N, Moriconi F, Ahmad S, Amanzada A, Khan S, Mihm S, Ramadori G and Malik IA. Fer-

ritin L is the sole serum ferritin constituent and a positive hepatic acute-phase protein. Shock 2013; 39: 520-526.

[18] Ahmad S, Moriconi F, Naz N, Sultan S, Sheikh N, Ramadori G and Malik IA. Ferritin L and Ferritin H are differentially located within hepatic and extra hepatic organs under physiological and acute phase conditions. Int J Clin Exp Pathol 2013; 6: 622-629.

[19] Amanzada A, Moriconi F, Mansuroglu T, Cameron S, Ramadori G and Malik A. Induction of chemokines and cytokines before neutrophils and macrophage recruitment in different regions of rat liver after TAA administration. Lab Invest 2014; 94: 235-47.

[20] Lauzier B, Merlen C, Vaillant F, McDuff J, Bouchard B, Beguin PC, Dolinsky VW, Foisy S, Villeneuve LR, Labarthe F, Dyck JR, Allen BG, Charron G and Des RC. Post-translational modifications, a key process in CD36 function: lessons from the spontaneously hypertensive rat heart. J Mol Cell Cardiol 2011; 51: 99-108.

[21] DiDonato JA, Mercurio F and Karin M. NF-kappaB and the link between inflammation and cancer. Immunol Rev 2012; 246: 379-400.

[22] Gruarin P, Sitia R and Alessio M. Formation of one or more intrachain disulphide bonds is required for the intracellular processing and transport of CD36. Biochem J 1997; 328: 635-642.

[23] Pan CC, Kavanagh BD, Dawson LA, Li XA, Das SK, Miften M and Ten Haken RK. Radiation-associated liver injury. Int J Radiat Oncol Biol Phys 2010; 76: S94-100.

[24] Tiniakos DG, Vos MB and Brunt EM. Nonalcoholic fatty liver disease: pathology and pathogenesis. Annu Rev Pathol 2010; 5: 145-171.

[25] Buettner R, Parhofer KG, Woenckhaus M, Wrede CE, Kunz-Schughart LA, Scholmerich J and Bollheimer LC. Defining high-fat-diet rat models: metabolic and molecular effects of different fat types. J Mol Endocrinol 2006; 36: 485-501.

[26] Nguyen P, Leray V, Diez M, Serisier S, Le BJ, Siliart B and Dumon H. Liver lipid metabolism. J Anim Physiol Anim Nutr (Berl) 2008; 92: 272-283.

[27] Abu-Elheiga L, Wu H, Gu Z, Bressler R and Wakil SJ. Acetyl-CoA carboxylase 2-/- mutant mice are protected against fatty liver under high-fat, high-carbohydrate dietary and de novo lipogenic conditions. J Biol Chem 2012; 287: 12578-12588.

[28] Degrace P, Moindrot B, Mohamed I, Gresti J, Du ZY, Chardigny JM, Sebedio JL and Clouet P. Upregulation of liver VLDL receptor and FAT/CD36 expression in LDLR-/- apoB100/100 mice fed trans-10,cis-12 conjugated linoleic acid. J Lipid Res 2006; 47: 2647-2655.

[29] Grefhorst A, Elzinga BM, Voshol PJ, Plosch T, Kok T, Bloks VW, van der Sluijs FH, Havekes LM, Romijn JA, Verkade HJ and Kuipers F. Stimulation of lipogenesis by pharmacological activation of the liver X receptor leads to production of large, triglyceride-rich very low density lipoprotein particles. J Biol Chem 2002; 277: 34182-34190.

[30] Motojima K, Passilly P, Peters JM, Gonzalez FJ and Latruffe N. Expression of putative fatty acid transporter genes are regulated by peroxisome proliferator-activated receptor alpha and gamma activators in a tissue- and inducer-specific manner. J Biol Chem 1998; 273: 16710-16714.

[31] Oyama Y, Takeda T, Hama H, Tanuma A, Iino N, Sato K, Kaseda R, Ma M, Yamamoto T, Fujii H, Kazama JJ, Odani S, Terada Y, Mizuta K, Gejyo F and Saito A. Evidence for megalin-mediated proximal tubular uptake of L-FABP, a carrier of potentially nephrotoxic molecules. Lab Invest 2005; 85: 522-531.

[32] Coe NR and Bernlohr DA. Physiological properties and functions of intracellular fatty acid-binding proteins. Biochim Biophys Acta 1998; 1391: 287-306.

[33] Koonen DP, Jacobs RL, Febbraio M, Young ME, Soltys CL, Ong H, Vance DE and Dyck JR. Increased hepatic CD36 expression contributes to dyslipidemia associated with diet-induced obesity. Diabetes 2007; 56: 2863-2871.

[34] Gupta D, Arora R, Garg AP, Bala M and Goel HC. Modification of radiation damage to mitochondrial system in vivo by Podophyllum hexandrum: mechanistic aspects. Mol Cell Biochem 2004; 266: 65-77.

[35] Perez-Carreras M, Del HP, Martin MA, Rubio JC, Martin A, Castellano G, Colina F, Arenas J and Solis-Herruzo JA. Defective hepatic mitochondrial respiratory chain in patients with nonalcoholic steatohepatitis. Hepatology 2003; 38: 999-1007.

[36] Rector RS, Thyfault JP, Uptergrove GM, Morris EM, Naples SP, Borengasser SJ, Mikus CR, Laye MJ, Laughlin MH, Booth FW and Ibdah JA. Mitochondrial dysfunction precedes insulin resistance and hepatic steatosis and contributes to the natural history of non-alcoholic fatty liver disease in an obese rodent model. J Hepatol 2010; 52: 727-736.

[37] Akkaoui M, Cohen I, Esnous C, Lenoir V, Sournac M, Girard J and Prip-Buus C. Modulation of the hepatic malonyl-CoA-carnitine palmitoyltransferase 1A partnership creates a metabolic switch allowing oxidation of de novo fatty acids. Biochem J 2009; 420: 429-438.

[38] Bruce CR, Hoy AJ, Turner N, Watt MJ, Allen TL, Carpenter K, Cooney GJ, Febbraio MA and

Kraegen EW. Overexpression of carnitine palmitoyltransferase-1 in skeletal muscle is sufficient to enhance fatty acid oxidation and improve high-fat diet-induced insulin resistance. Diabetes 2009; 58: 550-558.

[39] Jambor de Sousa UL, Koss MD, Fillies M, Gahl A, Scheeder MR, Cardoso MC, Leonhardt H, Geary N, Langhans W and Leonhardt M. CPT1alpha over-expression increases long-chain fatty acid oxidation and reduces cell viability with incremental palmitic acid concentration in 293T cells. Biochem Biophys Res Commun 2005; 338: 757-761.

[40] Reddy JK and Rao MS. Lipid metabolism and liver inflammation. II. Fatty liver disease and fatty acid oxidation. Am J Physiol Gastrointest Liver Physiol 2006; 290: G852-G858.

[41] Karin M and Gallagher E. TNFR signaling: ubiquitin-conjugated TRAFfic signals control stop-and-go for MAPK signaling complexes. Immunol Rev 2009; 228: 225-240.

[42] Takahashi Y, Soejima Y and Fukusato T. Animal models of nonalcoholic fatty liver disease/nonalcoholic steatohepatitis. World J Gastroenterol 2012; 18: 2300-2308.

[43] Alwahsh SM, Xu M, Schultze FC, Wilting J, Mihm S, Raddatz D, Ramadori G. Combination of alcohol and fructose exacerbates metabolic imbalance in terms of hepatic damage, dyslipidemia, and insulin resistance in rats. PLoS One 2014; 9: e104220.

[44] Alwahsh SM, Xu M, Seyhan HA, Ahmad S, Mihm S, Ramadori G, Schultze FC. Diet high in fructose leads to an overexpression of lipocalin-2 in rat fatty liver. World J Gastroenterol 2014; 20: 1807-21.